Enhanced degree of temporal coherence through temporal and spatial phase coupling within a focused supercontinuum

Brendan J. Chick, James W.M. Chon, and Min Gu

Centre for Micro-Photonics, Faculty of Engineering and Industrial Sciences, Swinburne University of Technology, P.O. Box 218, Hawthorn, 3122, Victoria, Australia.

mgu@swin.edu.au

Abstract: In the diffraction of a supercontinuum source, a redistribution of amplitude and phase at the focal region is incurred by the coupling between the supercontinuum and the spatial phase caused by the lens diffraction, making it extremely difficult to predict the focal behaviour. We show that the coupling between the temporal phase of a SC source and the spatial phase from the diffraction by a low numerical aperture (NA) lens causes dramatic alterations in the spectra and the temporal coherence near the focal region, and that this effect is maximized in points of singularity. Furthermore, we show that such an enhancement in temporal coherence can be controlled by the pulse evolution through the photonic crystal fiber, in which nonlinear and disperive effects such as the soliton fission process provides the key phase evolution necessary for dramatically changing the coherence time of the focused electromagnetic wave.

OCIS codes: (050.0050) Diffraction and gratings; (190.0190) Nonlinear optics; (260.0260) Physical optics; (030.0030) Coherence and statistical optics.

References and links

1. J. C. Knight, J. Broeng, T. A. Birks and P. St. J. Russell, "Photonic band cap guidance in optical fibers," Science **282**, 1476-1478 (1998).
2. J. K. Ranka, R. S. Windeler and A. J. Stentz, "Visible continuum generation in air-silica microstructure optical fibers with anomalous dispersion at 800 nm," Opt. Lett. **25**, 25-27 (2000).
3. I. Hartl, X. D. Li, C. Chudoba, R. K. Ghanta, T. H. Ko, J. G. Fujimoto, J. K. Ranka, and R. S. Windeler, "Ultrahigh-resolution optical coherence tomography using continuum generation in an air-silica microstructure fiber," Opt. Lett. **26**, 608–610 (2001).
4. H. N. Paulsen, K. M. Hilligsøe, J. Thøgersen, S. R. Keiding, and J. J. Larsen, "Coherent anti-Stokes Raman scattering microscopy with a photonic crystal fiber based light source," Opt. Lett. **28**, 1123–1125 (2003).
5. Th. Udem, R. Holzwarth, and T. W. Hänsch, "Optical frequency metrology," Nature **416**, 233–237 (2002).
6. J. E. Morris, A. E. Carruthers, M. Mazilu, P. J. Reece, T. Cizmar, P. Fischer and K. Dholakia, "Optical micro-manipulation using supercontinuum Laguerre Gaussian and Gaussian beams," Opt. Express **16**, 1011–10129 (2008).
7. W. H. Reeves, D. V. Skryabin, F. Biancalana, J. C. Knight, P. St. J. Russell, F. G. Omenetto, A. Efimov and A.J. Taylor, "Transformation and control of ultrashort pulses in dispersion-engineered photonic crystal fibers," Nature **474**, 511–515 (2003).
8. A. V. Husakou and J. Herrmann, "Supercontinuum generation higher-order solutions by fission in photonic crystal fibers," Phys. Rev. Lett. **87**, 203901 (2001).
9. J. M. Dudley, G. Genty and S. Coen, "Supercontinuum generation in photonic crystal fiber," Mod. Phys. Rev. **78**, 113–1184 (2006).

10. F. De Martini, C. H. Townes, T. K. Gustafson, and P. L. Kelley, "Self-Steepening of light pulses," Phys. Rev. **164**, 312-323 (1967).
11. C.V. Raman, "A change of wave-length in light scattering [8]," Nature **121**, 619- (1928).
12. K. B. Shi, P. Li, S. Z. Yin and Z. W. Liu, "Chromatic confocal microscopy using supercontinuum light," Opt. Express **12**, 2096-2101 (2004).
13. K. Isobe, W. Watanabe, S. Matsunaga, T. Higashi, K. Fukui and K. Itoh, "Multi-spectral two-photon excited fluorescence microscopy using supercontinuum light source," Jpn. J. Appl. Phys. **44**, L167-L169 (2005).
14. M. Born and E. Wolf, "Principles of Optics," 7th ed. (Cambridge University Press, Cambridge, 1999).
15. G. Gbur, T. D. Visser and E. Wolf, "Anomalous behavior of spectra near phase singularities of focused waves," Phys. Rev. Lett. **88**, 013901 (2002).
16. D. W. Robinson and G. T. Reid, "Phase unwrapping methods," Interferogram Analysis, 194-229 (1993).
17. W. Wang, N. Ishii, S. G. Hanson, Y. Miyamoto and M. Takeda, "Phase singularities in analytic signal of white-light speckle pattern with application to micro-displacement measurement," Opt. Comm. **248**, 59-68 (2005).
18. M. Gu, "Advanced optical imaging theory," (Springer Velag, Heidelberg, 2000).
19. B. J. Chick, J. W. M. Chon and M. Gu, "Polarization effects in a highly birefringent nonlinear photonic crystal fiber with two-zero dispersion wavelengths," Opt. Express **16**, 20099-20080 (2008).
20. R. Loudon, "The quantum theory of light," 2nd ed. (Oxford University Press, 1983).
21. M. Bertolotti, A. Ferrari and L. Sereda, "Coherence properties of nonstationary polychromatic light sources," J. Opt. Soc. Am. B **12**, 341-347 (1995).
22. L. Sereda and M. Bertolotti, "Coherence properties of nonstationary light wave fields," J. Opt. Soc. Am. A **15**, 695-705 (1998).
23. G. P. Agrawal, "Nonlinear fiber optics," 3rd ed. (Academic San Diego, Calif., 2002).
24. K. L. Corwin, N. R. Newbury, J. M. Dudley, S. Coen, S. A. Diddams, K. Weber and R. S. Windler, "Fundamental noise limitations to supercontinuum generation in microstructured fiber," Phys. Rev. Lett. **90**, 112904 (2003).
25. J. M. Dudley and S. Coen, "Coherence properties of supecontinuum sprectra generated in photonic crystal and tapered optical fibers," Opt. Exp. **27**, 1180-1182 (2002).

1. Introduction

Over the past decade supercontinuum (SC) generation by micro-structured optical fiber [1, 2] has become an imperative instrument for many applications [3–6] involving the diffraction by an objective lens. SC generation in micro-structured optical fiber [1, 2] is a construction of broadband light by modifying the phase of an ultrashort pulse through the interplay between the nonlinearity induced by the Kerr effect and the tailored modal dispersion [7]. When an ultrashort pulse enters a micro-structured fiber the initial phase contributions are self phase modulation, second order dispersion and third order dispersion. The ultrashort pulse forms a higher order soliton which begins fissions into fundametal solitons [8] at a particular point during propagation [9]. Other effects such as self steepening [10] and Raman scattering [11] contribute to the temporal phase through higher order oscillating phase terms. These effects then combine to form a complex temporal phase field depending on the length of the optical fiber [9]. Due to its spectral extent and ultrashort temporal features, SC is the ideal instrument for many forms of microscopy such as optical coherence tomography (OCT) [3], coherent anti-Stokes Raman scattering microscopy (CARS) [4], confocal microscopy [12], two-photon microscopy [13] and laser tweezing under a microscope [6]. SC provides the capability of simultaneous optical imaging with multiple frequencies to develop an understanding of the molecular dynamics of chemical or biological samples.

However, when a polychromatic wave is focused, the diffraction condition enforced by the lens needs to be considered rigorously to predict the characteristics of its focus. The diffraction of a polychromatic wave such as a SC wave is described by what is known as the Huygen-Fresnel principle [14] where the incoming wave produces a set of secondary wavelets which superimpose and mutually interfere. The spatial phase associated with the diffraction caused by a circular lens transforms the polychromatic wave to form an Airy pattern. At particular points in the diffraction field the superposition of these wavelets produces discontinuities in phase, known as singular points for each frequency. In recent years it has been shown that when light of a finite bandwidth is focused by a lens of low NA, the distribution of intensity is

altered and its spectrum is split by these phase singularities [15], which has led to optical vortex metrology [16, 17] for phase unwrapping.

Physically, the addition of temporal phase onto an electromagnetic wave can change the superposition condition of the focal distribution. Since there exists a temporal and spatial phase coupling through the wavefront propagation, it is intuitive that a temporal phase variation of SC would affect the diffraction by the lens. What is presented in this article is the coupling relationship between the temporal and spatial phase within a focused SC, and how the diffraction modification through phase singularities enhances the degree of temporal coherence of a SC in the focal region.

2. Supercontinuum diffraction

The diffraction of a polychromatic wave such as a SC wave is calculated using the scalar diffraction theory, which can be given, under the paraxial approximation, by [18]

$$U_1(u,v,\omega) = -\frac{i\omega NA^2}{c} e^{iu/NA^2} \int_b^a U(\omega) J_0(v\rho) e^{-\frac{1}{2}iu\rho^2} \rho \, d\rho \qquad (1)$$

The dimensionless parameters u and v are given by $u = \frac{\omega}{c}(NA)^2 z$ and $v = \frac{\omega}{c}(NA) r$ respectively, where r and z are the radial and axial coordinated of the lens image space. The parameter a and b are the aperture radius and the integral lower bound for the lens, NA is the numerical aperture, J_0 is a zero order Bessel function of the first kind, ω is the angular frequency and c is the speed of light. If $b = 0$, the diffraction is for the complete aperture and for a non zero b is a diaphragm. $U(\omega)$ is the Fourier transform of the SC wave using the dispersion parameters, nonlinear parameters and the method described by *Chick et. al.* [19], and the Fourier transform of $U_1(u,v,\omega)$ is used to obtain the temporal profile $U_1(u,v,t)$.

An analytic solution ($v = 0$) for the diffraction field [Eq. (1)] can be obtained by the following equation:

$$U_1(u,v,\omega) = -\frac{\omega NA^2}{uc} U(\omega) e^{iu/NA^2} \left(e^{-\frac{1}{2}ib^2 u} - e^{-\frac{1}{2}ia^2 u} \right) \qquad (2)$$

From Eq. (2) it can be seen that when $a^2 u/2 = \pm 2n\pi$ and if $b = 0$, the equation is equal to $\frac{0}{u}$ which is a singularity. Since u is dependent on both ω and z there lays a region of singularity.

As the SC electromagnetic field propagates through a lens it is diffracted and modified through the spatial phase of the wavefront. The superposition of the wavefront from the outer aperture to the inner aperture has an inherent path difference (Fig. 1a), which mutually interferes. The destructive interference at certain frequency components of the SC wave produces a singularity. These points occur at discrete positions in both the axial and radial directions and can be determined through the parameter $u = \frac{\omega}{c}(NA)^2 z$ and occur at $u = \pm 4n\pi$ (where n is an integer, for the radial direction is the zero of a zero order Bessel function of the first kind). The parameters u_0 and v_0 (Fig. 1a) are defined as the normalized axial and radial coordinates of the optical system and are given by $u_0 = \frac{2\pi}{\lambda_0}(NA)^2 z$ and $v_0 = \frac{2\pi}{\lambda_0}(NA) r$, where NA is the numerical aperture, z and r are the axial and radial dimensions (in μm), and λ_0 is the center wavelength of the original pulse coupled to the nonlinear photonic crystal fiber (the input pulse is a hyperbolic secant pulse which is used to represent a mode-locked laser pulse).

The analysis used to understand how a SC propagates through the focal region depends on the method of its detection or observation (Fig. 1b). In a conventional optical system with a single point detector, the intensity that is collected depends on the diffraction for an axial (and radial) position (stationary observer, $S(t,z_0)$) and evolves with time. The intuitive observation however would be to view the focal plane from the side, where the intensity is both temporally
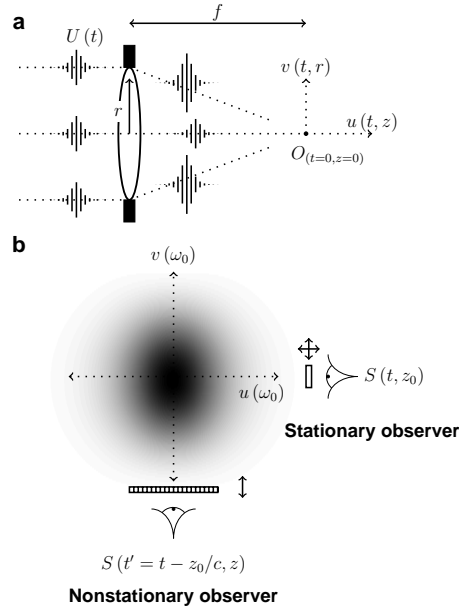
Fig. 1. An illustration of pulse diffraction by a low NA lens. (a) shows how the path length and the NA affect the pulse distribution as the temporal envelope passes through the focus. (b) shows the observation frames of the intensity profile in the focus.

and axially dependent since the leading intensities of the pulse are modified by the diffraction for an axial position and differs from the trailing intensities ($S(t,z)$), which is referred to as a nonstationary observer. $U(\omega)$ is the intensity distribution for the stationary observation frame where the intensity for the nonstationary observation frame is obtained by taking the diagonal of the the matrix $U_1(u,t)$ for different v.

The influence of the lens results in a superposition of amplitude and phase which determines the diffracted focal distribution (Fig. 2a). Since the SC field contains structured temporal components, as it encounters singularities it is expected that the temporal modification would be more significant. If the frequency distribution of a temporal field coincides with the frequency dependence of the singularities, a pulsed feature would be removed (Fig. 2b). Since there is a path difference incurred across the aperture and an increased temporal and spectral extent of the SC, the diffraction in the focal plane is more dramatic (Fig. 2c). The focal distribution on the axis (Fig. 2d) shows the complexity of singularities of the lens diffraction and how they manipulate the SC field temporal structure.

3. Temporal coherence and mean frequency

The modification of the temporal and spatial behavior of a focused SC wave can be characterized through the degree of coherence ($g^1(u_0, v_0, \tau)$) which is generalized through the correlation between two points and is calculated by [20]

$$g^1(z_1, t_1 : z_2, t_2) = \frac{\langle U^*(z_1, t_1) U(z_2, t_2) \rangle}{[\langle |U(z_1, t_1)|^2 \rangle \langle |U(z_2, t_2)|^2 \rangle]^{\frac{1}{2}}} \tag{3}$$

where z and t are the axial and temporal coordinates.
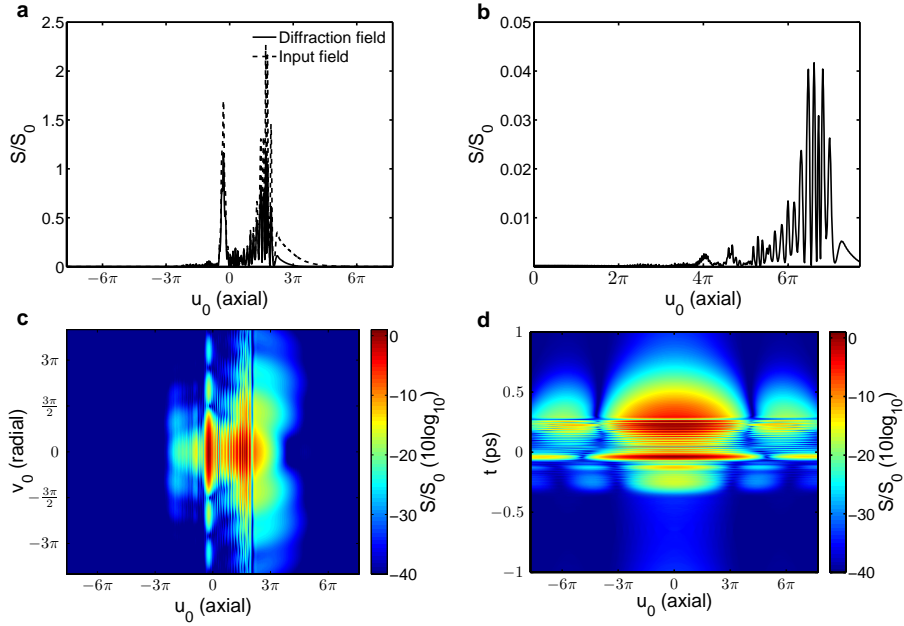
Fig. 2. The temporal effects of a SC propagating through the focus of a low NA (0.1) objective. (a) On axis diffraction centered at the focal point (the full temporal evolution of the SC on the axis can be viewed from the supplementary Media 1). (b) On axis diffraction centered at $u_0 = 5\pi$. (c) Radial and axial diffraction pattern centered at the focal point (the full temporal evolution of the SC in the radial and axial direction can be viewed from the supplementary Media 2). (d) Complete axial and temporal diffraction field. The SC field was calculated with a peak power of 2500W and a pulse width of 0.1ps with the dispersion and nonlinear parameters as described by *Chick et. al.* [19].

For a stationary beam (e.g. in a Mach Zehnder interferometer) within the diffraction field, the spatial paramters u_0 and v_0 remain constant; hence Eq. (3) becomes an auto-correlation technique determined by

$$g^1(u_0, v_0, \tau) = \frac{\langle U_1^*(u_0, v_0, t), U_1(u_0, v_0, t+\tau) \rangle}{\langle U_1(u_0, v_0, t), U_1(u_0, v_0, t) \rangle} \tag{4}$$

$g^1(u_0, v_0, \tau)$ depends on the position (u_0, v_0) of the detector.

However, when considering the wave packet (in a nonstationary observational frame) the calculation becomes spatiotemporal and is given by [20]

$$g^1(u_0, v_0, \tau) = \frac{\langle U_1^*(u, v_0, t) U_1(u+u_0, v_0, t+\tau) \rangle}{\left[\langle |U_1(u, v_0, t)|^2 \rangle \langle |U_1(u+u_0, v_0, t+\tau)|^2 \rangle \right]^{\frac{1}{2}}} \tag{5}$$

where the variables u_0 and τ are related by $c = u_0/\tau$. This nonstationary frame of reference has been investigated for nonstationary polychromatic waves [21, 22]. Using Eq's. (4) and (5) the coherence time for the field can be calculated through [20]

$$\tau_c(u_0, v_0) = \int_{-\infty}^{\infty} |g^1(u_0, v_0, \tau)|^2 d\tau \tag{6}$$

The correlation function of a field point essentially provides a measure of the frequency component variation. The degree of coherence within a focused SC field is expected to vary dramatically due to the removal of frequencies within the temporal profile caused by the singularity and is quantified through the coherence time τ_c (Figs. 3a-d) using Eq. (6). For the stationary observation frame, the coherence time changes around the region of the phase singularity (Fig. 3a) and in fact an enhancement of the coherence time occurs because of the spectral redistribution that modifies the bandwidth. Compared with the coherence time, $\tau_0 = 0.005\,ps$, of the SC before it is focused, τ_c at the singularities is enhanced by a factor of 2. The coherence time in this situation is symmetric with respect to the focal plane, which is physically expected since it is contributed by a single axial position. In this case, the spatial phase contribution from the lens diffraction is unchanged during the correlation measurement, since the diffraction equation is symmetric with respect to the focal plane. This symmetry holds for larger NA lenses and thus the coherence time shows little variation with NA (Fig. 3c).
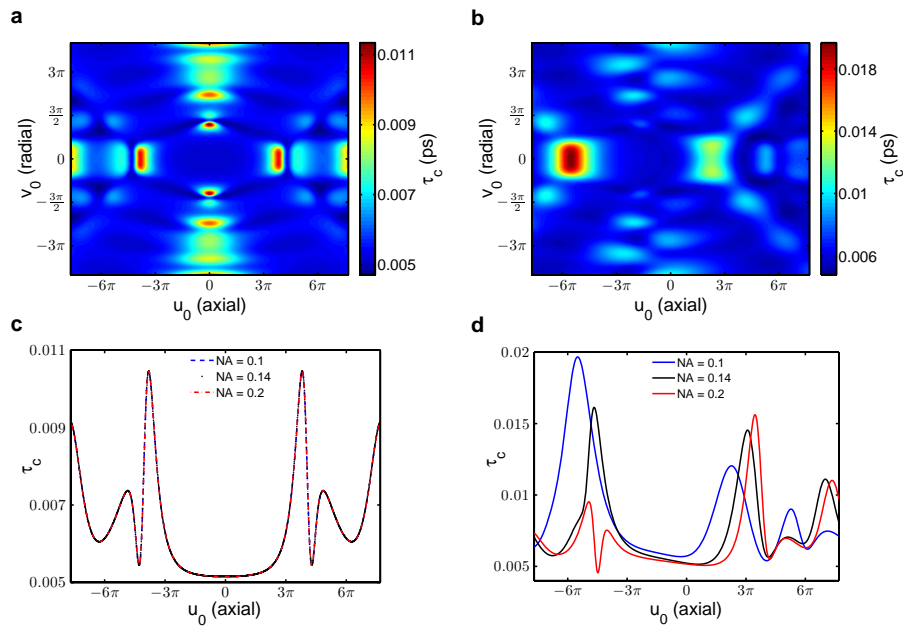
Fig. 3. The coherence time within a focused SC for the stationary and the non-stationary cases. (a) Axial and radial distribution of the coherence time for the 0.1 NA lens for the stationary case; (b) Axial and radial distribution of the coherence time for the 0.1 NA lens for the non-stationary case; (c) Effect of NA on the coherence time on the axis for the stationary case; and (d) Effect of NA on the coherence time on the axis for the non-stationary case.

However, depending on the observational view the calculated coherence time is different. For the nonstationary observation frame (e.g. in a time resolved experiment), the coherence time shows a remarkable difference (Fig. 3b) and is caused by the path difference incurred by the rays which pass the extremities of the lens compared to rays on the optical axis. Further, the path difference is not symmetric with respect to the focal plane. This effect can be confirmed by changing the NA (Fig. 3d) where the coherence time changes dramatically. Such an effect leads to the enhancement of the coherence time by a factor 4 near the singularity before the focal

plane. This effect occurs because of the variation of the path difference through the focal plane and the change in sign of the spatial phase on either side of the focus. Though both observational frames are valid in a laboratory measurement, the nonstationary observation frame has greater consequences. The coherence time is strongly dependent on the temporal variance of the input field as well as the spatial phase contribution from the lens diffraction. This effect would have a strong impact on time resolved (or frequency resolved) measurements and would rely on the characteristics of the SC and the NA of the lens.
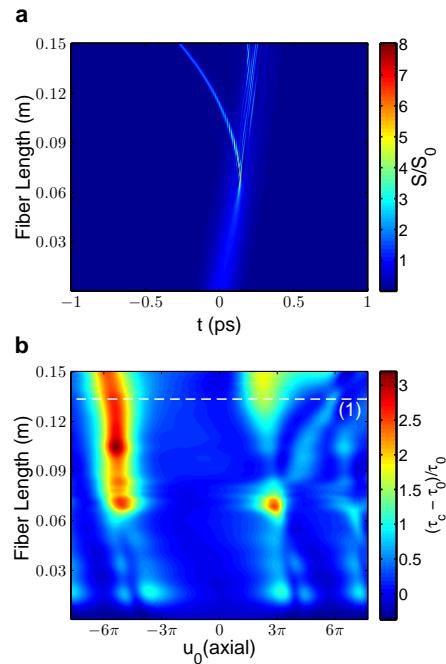
Fig. 4. Propagation of an ultrashort hyperbolic secant pulse through a nonlinear photonic crystal fiber. (a) field propagation as a function of fiber length (b) coherence time in the focal region for different length fiber. The peak input power to the photonic crystal fiber is 2500W with a pulse duration of 100fs. (1) represents the cross section used for Fig. 3d (blue).

The phase on the SC temporal profile is dependent on the physical origin of nonlinear and dispersive effects that occur because of the nonlinear photonic crystal fiber (PCF). The dominant effect in the initial pulse propagation through a PCF is the balance between self phase modulation and second order dispersion, as the pulse proceeds further into the fiber dispersive effects become more dominant (Fig. 4a). The ultrashort pulse initially forms a higher order soliton and at a particular point in the propagation, fissions into many fundamental solitons. The phase contribution caused by these effects can be isolated by observing the coherence time in the diffraction of a lens using an input field generated by a PCF with varying length. Initially, the temporal coherence behaves similar to a chirped hyperbolic secant pulse shape (partially coherent source) with a predictable structure, but at a particular length corresponding to the fission length of the higher order soliton the coherence time dramatically changes. This observation confirms that an increase in phase complexity added to the original ultrashort pulse (with linear phase [23]) is coupled with the spatial phase from the lens diffraction to modify

the correlation of the electromagnetic field.

Statistically, SC generation varies from pulse to pulse due to fluctuations created by noise [24,25] such as spontaneous Raman scattering. The correlation and therefore the coherence time in the focus would also vary at the single pulse level. However, since the majority of applications involving a SC involve the ensemble measurement, these fluctuations would average out and should result in minimal fluctuations in the coherence time.
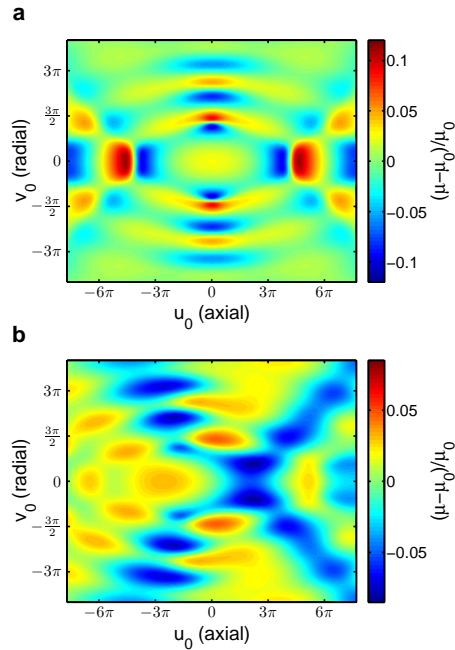
Fig. 5. Mean frequency distribution of the focused SC in the axial and radial plane of a 0.1 NA lens for stationary (a) and non-stationary (b) cases.

Physically, the temporal coherence of a field is related to the bandwidth Δv by $\tau_c = 1/\Delta v$. Though the definition of the bandwidth is not straightforward in the case of singularity, the mean frequency μ, introduced previously for the description of focusing a polychromatic wave [15], can be used to confirm the temporal correlation and relative frequency shifting of the focused SC wave. From both observational frames, the mean frequency would be related to the inverse of its temporal coherence (Fig. 5). For a SC it is expected that the frequency shifting would be much broader due to the increase in bandwidth. Since the increase in bandwidth results in a wider region of singular points, it is also expected that the spatial location of spectral shifting would be broader. However, Fig. 5a shows a behavior which is different from what is seen in previous literature [15]. The frequency shifting in the radial plane from the focal point moving radially outward becomes less profound. The superposition of the diffraction field and the input SC in this region makes the bandwidth narrower, causing a reduction in the magnitude of the mean frequency. Specifically, for the stationary observation frame (Fig. 5a) the mean frequency is symmetric about the focal point which is due to the symmetric nature of the diffraction process and the spatial phase contribution remains constant. However, for the nonstationary observation frame (Fig. 5b) the result becomes asymmetric because of the observed phenomenon in Fig. 3b.

4. Conclusion

To summarize, we have demonstrated the coupling of temporal and spatial phases that arise from the diffraction of a SC by a lens. The contribution of temporal phase from the input source superimposes with the diffraction field of a low NA lens to modify the bandwidth of the input which alters its correlation. At a particular point where soliton fission occurs in the pulse evolution through the PCF, the correlation changes from being easily predicatable to a complex structure. These effects can be observed from two different observation frames which gives rise to the significantly different coherence times. Consequently, for a nonstationary observer with the addition of complex temporal input phase can enhance the coherence time by a factor of 3.

The alteration of bandwidth is extremely important and would change the excitation frequency range that can be applied in microscopy applications involving multiple wavelength excitation. The surprising effects on the bandwidth and temporal correlation at points of singularity could provide interesting dynamics for applications such as optical vortex metrology where these singular regions provide signatures for phase unwrapping. In all these applications, the SC source provides the capability to tailor the temporal coherence and bandwidth within the focal region for a particular application.